Follicular T cells and tissue IgG3 or IgG4 expressing plasma cells in a case of IgG4-related systemic disease with interstitial nephritis

Mohamad Zaidan, Pascale Cervera-Pierot, Sophie de Seigneux, Karine Dahan, Bettina Fabiani, Patrice Callard, Pierre Ronco, Pierre Aucouturier

Follicular T cells and tissue IgG3 or IgG4 expressing plasma cells in a case of IgG4-related systemic disease with interstitial nephritis

Mohamad Zaidan[1], Pascale Cervera-Pierot[2, 3]*, *MD, PhD*, Sophie de Seigneux[1]*, *MD*, *PhD*, Karine Dahan[1], *MD*, Bettina Fabiani[2], *MD*, Patrice Callard[3, 4], *MD*, Pierre Ronco[1, 3, 5]*, *MD*, *PhD*, and Pierre Aucouturier[3, 6]*, *PhD*.

* Equal contribution

[1] AP-HP, Hôpital Tenon, Service de Néphrologie et Dialyses, F-75020, Paris, France

[2] AP-HP, Hôpital St Antoine, Service d'Anatomie et cytologie pathologiques, F-75012, Paris, France

[3] UPMC Univ – Paris 6, F-75020, Paris, France

[4] AP-HP, Hôpital Tenon, Service d'Anatomie pathologique, F-75020, Paris, France

[5] INSERM UMR_S 702, F-75020, Paris, France

[6] INSERM, UMR_S 938, F-75012, Paris, France

Correspondence to: Pierre Aucouturier**,** INSERM UMR S 938, Hôpital St-Antoine, 184 rue fbg St-Antoine, F-75012 Paris, France. Tel.# +33 1 4344 3442. Fax # +33 1 4340 1748

E-mail: pierre.aucouturier@inserm.fr

Keywords: IgG4-related systemic disease, IgG4, follicular helper T cells, lymphadenopathy, rituximab, tubulointerstitial nephritis.

SUPPORT: No outside funding

FINANCIAL DISCLOSURE DECLARATION: The authors declare no relevant financial interests.

ABSTRACT

An 83-year-old man presented with weight loss, lymphadenopathies, anicteric cholestasis, and a striking hypergammaglobulinemia. He developed renal failure with tubular proteinuria. Investigations revealed pronounced increase of serum polyclonal IgG1, IgG3 and IgG4, and salivary gland and kidney interstitium infiltrates that included B-lymphocytes, T-lymphocytes and IgG3+ and IgG4+ plasma cells. Remarkably, lymph node B-cell follicles germinal centers were invaded by numerous T-cells, mostly CD4+. The diagnosis was IgG4-related systemic disease. Rituximab (375 mg/m²/week for 4 weeks) induced a dramatic and sustained clinical and biological improvement.

To date, very little is known on the mechanisms underlying IgG4-related systemic disease. In addition to perfectly illustrate the broad spectrum of this protean condition, the present case provides further insights on its pathophysiology. The efficacy of rituximab suggests a critical role of CD20+ B-cells in the disease clinical expression and progression. The overexpression of IgG1 and IgG3, in addition to IgG4, and the unusual abundance of CD4+ T-cells in germinal centers of the B-cell follicles points to a possible role of B follicular helper T-cells in enhancing a skewed B-cell terminal maturation.

INTRODUCTION

IgG4-related systemic disease (IgG4-RSD) is currently recognized worldwide as a single and enigmatic condition (1). This protean disorder covers an increasing variety of lesions including the so-called “autoimmune pancreatitis" (1-6). Renal involvement, which mainly relates to interstitial nephritis, has been recently characterized (7). Little is known yet about the underlying mechanisms, and few reports have systematically studied all IgG subclasses and evoked the possible implication of T-cells (4,5). We describe an observation of IgG4-RSD that suggests a role of follicular helper T cells in enhanced terminal B-cell maturation.

CASE REPORT

An 83 year-old Chinese man, with a history of pulmonary tuberculosis and 60 pack-year smoking, was hospitalized for progressive dyspnea, a 12 kg weight loss, and abdominal pain. Physical examination was remarkable for bilateral crackles and slightly swollen inguinal lymph nodes. Laboratory tests revealed: aspartate aminotransferase 69 U/L alanine aminotransferase 64 U/L, alkaline phosphatase 365 U/L, gamma-glutamyltransferase 203 U/L, serum creatinine (1.06 mg/dL (94 µmol/L), estimated glomerular filtration rate (eGFR) 66 mL/min/1.73 m² (1.1 mL/s/1.73 m²) according to 4-variable Modified of Diet in Renal Disease (MDRD) Study equation), normal levels of bilirubin, lipase, CRP, and lactate dehydrogenase. Serum protein electrophoresis showed a diffuse hypergammaglobulinemia (5.2 g/dL (52 g/L)). Chest computed tomography scan revealed lung parenchyma changes and lymphadenopathies. Sputum and bronchoscopic aspirate smears were negative for acid-fast bacilli. Abdominal computed tomography scan showed biliary tree enlargement. Endoscopic ultrasonography showed a pancreas of heterogeneous echostructure. The main bile duct was enlarged, with a stricture just above the papilla. A sphincterotomy was performed.

Three months later, the patient reported mild xerostomia. Minor salivary gland biopsy showed a dense infiltration of lymphocytes and plasma cells, with periductal fibrosis. Serum creatinine increased to 1.58 mg/dL (140 µmol/l, eGFR 42 mL/min/1.73 m² (0.7 mL/s/1.73 m²)). The patient was referred for persistent renal failure.

Examination disclosed a further 7 kg weight loss and axillary and inguinal lymphadenopathies. Renal ultrasound showed normal-sized kidneys but mild left hydronephrosis, which did not require ureteral endoprothesis. Magnetic resonance imaging confirmed local retroperitoneal fibrosis. Laboratory data are summarized in **Table 1**. Urinalysis revealed a tubular proteinuria (1.5 g/day) but neither hematuria nor leukocyturia. Anicteric cholestasis and bile duct enlargement were still observed. TSH level was increased. Antinuclear antibodies were positive (>1:1280). Anti-smooth-muscle and antineutrophil cytoplasmic antibodies with anti-MPO specificity were also positive. However, testing for antibodies to double-stranded DNA, ENA including SSA and SSB, Liver/Kidney/Microsomes, and mitochondria, as well as rheumatoid factor and cryoglobulin, was negative. The hemolytic complement activity and components C3 and C4 were decreased to 3% (*NR*>50%), 0.25 mg/mL (*NR*=0.9-1.74 mg/mL) and <0.03 mg/mL (*NR*=0.22-0.51 mg/mL), respectively. Testing for HIV, hepatitis C virus, HTLV and HHV-8 was negative. Blood tests for hepatitis B virus, HHV-6, EBV and CMV indicated cured infections. There was a striking elevation of serum IgG (8100 mg/dL (81 g/L), *NR*=660-1240 mg/dL) and immunoglobulin free light chains *kappa* (1080 mg/L, *NR*=3.3-19.4 mg/L) and *lambda* (372 mg/L, *NR*=5.7-26.3 mg/L). Serum IgG subclasses measured by competitive ELISA with monoclonal antibodies (8) showed increased IgG1 (6000 mg/dL), IgG3 (1950 mg/dL) and IgG4 levels (1750 mg/dL), and normal IgG2 (330 mg/dL). Total IgE level was increased (1295 U/ml, *NR*<150 U/ml). Serum IgA level was normal (240 mg/dL (2400 mg/L), *NR*=101-320 mg/dL), IgM in the lower-normal range (52 mg/dL (520 mg/L), *NR*=48-137 mg/dL).

The axillary lymph node biopsy (**Figure 1A**) exhibited lymphoid follicular hyperplasia, and the remarkable presence of numerous plasma cells mainly in interfollicular zones. Upon immunostaining for intra-cytoplasmic IgG1, IgG2, IgG3 and IgG4 (monoclonal antibodies, clones 4E3, HP6014, ZG4 and MC011, respectively), almost all were IgG4+ (57%) or IgG3+ (42.8%). Another striking feature was the quite unusual abundance of CD4+ T-cells inside light zones of germinal centers, which was not found in controls. CD8+ cells were also found in germinal centers. The kidney biopsy (**Figure 1B**) displayed a heavy interstitial cellular infiltrate including B- and T-lymphocytes together with plasma cells, most of which stained for IgG3 (60.7%) and IgG4 (32.5%). Studies of the salivary gland biopsy (**Figure 1C**) also revealed abundant infiltrates of B-lymphocytes, T-lymphocytes and plasma cells that stained for IgG3 or IgG4 (42% and 44%, respectively).

In spite of distinctive features such as remarkably high serum levels of IgG1 and IgG3 in addition to IgG4, a diagnosis of IgG4-related systemic disease (IgG4-RSD) was retained because of dense IgG4+ plasma-cell infiltration of mildly swollen lymph nodes with follicular hyperplasia, tubulo-interstitial nephritis, lympho-plasmacytic sialadenitis, retroperitoneal fibrosis, bile duct involvement, and subclinical hypothyroidism.

While renal function improved, the patient remained extremely altered. In order to avoid the side effects of steroids in this elderly patient, we administered four weekly infusions of rituximab (375 mg/m²/week). The patient presented prompt clinical and biological improvement (**Table 1**).

DISCUSSION

We describe an elderly patient who presented with multi-organ involvement, polyclonal hypergammaglobulinemia, huge increase of serum IgG1, IgG3 and IgG4, and IgG3+ and IgG4+ plasma cell tissue infiltrates. Primary Sjögren's syndrome and other

autoimmune diseases, as well as infectious or lymphoproliferative conditions were ruled out. Altogether, IgG4-RSD brought unity to all observed manifestations. This protean condition is currently recognized worldwide and associates a broad spectrum of inflammatory and sclerosing lesions (**Table 2**) (1-7).

IgG4-RSD renal involvement mainly relates to tubulointerstitial nephritis with infiltration of lymphocytes and plasma cells that can lead to renal failure (7). So far, neither proximal nor distal tubular dysfunctions have been described. Glomerular involvement, particularly membranous nephropathy with IgG4 deposits, can occur in association with plasma-cell tubulointerstitial nephritis (7). It is noteworthy that IgG4 also predominates in idiopathic membranous nephropathy-related deposits. Kidney tumor-like lesions with dense IgG4+ plasma-cell infiltrate and other urological lesions have also been reported (2-7).

Steroids are the mainstay of IgG4-RSD treatment (4,9). There is no consensus on the overall duration of steroid treatment, but withdrawal should be attempted in controlled disease. Despite initial improvement, the long-term outcome remains uncertain and relapse occurs in 30-40% of cases (9). Only scarce data on the off-label use of rituximab in IgG4-RSD are available: patients who were refractory to steroids dramatically improved under anti-CD20 therapy (10,11). In the present case, rituximab induced a prompt and sustained improvement. This may be explained by the relatively numerous CD20+ infiltrating B-lymphocytes that might participate in the sclerosing process. However, long-term follow-up is necessary before considering rituximab as an alternative or complementary drug to steroids.

Although the present case is in line with the current description of IgG4-RSD, some unusual features may shed light on the pathophysiology. A direct role of IgG4 would be a priori surprising, as it has been characterized as an anti-inflammatory immunoglobulin isotype (12). Moreover, serum IgG4 level may be normal in well-characterized systemic sclerosing diseases and autoimmune pancreatitis (13). In our observation, IgG1 and IgG3 were elevated

together with IgG4 and IgE, and tissue infiltrating plasma cells mostly expressed IgG4 and IgG3. Hypocomplementemia and increased serum IgG3 seem more frequent in patients with interstitial nephritis in a recent series of 25 patients with IgG4-RSD (Mikael Ebbo *et al.*, submitted for publication). Interestingly, abundant T-cells in the germinal center of light zones relate either to an abnormal proliferation of follicular B helper T-cells (Tfh) or to the attraction of other T-cells into these regions that are specialized in B-cell terminal maturation and immunoglobulin class switch (5,14,15). The rapid decrease of IgG1, IgG3 and IgG4 serum levels after rituximab initiation suggests that B-cell activation by Tfh cells raises short-lived plasma cells. Enhanced T-B cooperation could result in skewed isotype switch, exacerbated B-cell proliferation and terminal maturation, and rapid turn-over of disease-associated plasma cells (4,10,16). A specific commitment to IgG1, IgG3 and IgG4 may result from cytokines such as IL-4, IL-10 and IL-21 that are classically produced by Tfh cells and may act as switch factors (4,12,14,16-19). Alternately, or in addition, other yet undefined anomalies upstream of B-cell maturation events could explain the bias in Ig isotypes (4,12,16).

In summary, renal manifestations clearly fall within the broad-spectrum of IgG4-RSD. The present case underscores that increased serum IgG4 level and infiltration by IgG4+ plasma cells may only reflect one of the imbalanced IgG isotypes. The dramatic effect of rituximab also points to a key role of CD20+ B-cells in disease progression and a possible enhancement of T-B cooperation as a key pathogenic process in IgG4-RSD. A careful analysis of infiltrating T- and B-cells, and cytokine profile, may provide further insights on class-switch process and B-cell terminal maturation and shed light on the yet undefined primary events underscoring this puzzling condition.

REFERENCE LIST

1. Kamisawa T, Funata N, Hayashi Y, et al. A new clinicopathological entity of IgG4-related autoimmune disease. *J Gastroenterol*. 2003;38:982-984.
2. Hamano H, Arakura N, Muraki T, Ozaki Y, Kiyosawa K, Kawa S. Prevalence and distribution of extrapancreatic lesions complicating autoimmune pancreatitis. *J Gastroenterol.* 2006;41:1197-1205.
3. Masaki Y, Dong L, Kurose N, et al. Proposal for a new clinical entity, IgG4-positive multiorgan lymphoproliferative syndrome: analysis of 64 cases of IgG4-related disorders. *Ann Rheum Dis.* 2009;68:1310-1315.
4. Park DH, Kim MH, Chari ST. Recent advances in autoimmune pancreatitis. *Gut.* 2009;58:1680-1689.
5. Cheuk W, Chan JK. IgG4-related sclerosing disease: a critical appraisal of an evolving clinicopathologic entity. *Adv Anat Pathol*. 2010;17:303-332.
6. Zen Y and Nakanuma Y. IgG4-related disease: a cross-sectional study of 114 cases. *Am J Surg Pathol.* 2010;34:1812-1819.
7. Saeki T, Nishi S, Imai N, et al. Clinicopathological characteristics of patients with IgG4-related tubulointerstitial nephritis. *Kidney Int.* 2010;78:1016-1023.
8. Aucouturier P, Mounir S, Preud'homme JL. Distribution of IgG subclass levels in normal adult sera as determined by a competitive enzyme immunoassay using monoclonal antibodies. *Diagn Immunol*. 1985;3:191-196.
9. Kamisawa T, Shimosegawa T, Okazaki K, et al. Standard steroid treatment for autoimmune pancreatitis. *Gut.* 2009;58:1504-1507.
10. Khosroshahi A, Bloch D, Deshpande V, Stone J. Rituximab therapy leads to rapid decline of serum IgG4 levels and prompt clinical improvement in IgG4-related systemic disease. *Arthritis Rheum*. 2010;62:1755-1762.
11. Topazian M, Witzig T, Smyrk T, et al. Rituximab therapy for refractory biliary strictures in immunoglobulin G4-associated cholangitis. *Clin Gastroenterol Hepatol*. 2008;6: 364-366.
12. Aalberse R, Stapel S, Schuurman J, Rispens T. Immunoglobulin G4: an odd antibody. *Clin Exp Allergy*. 2009;39:469-477.
13. Song TJ, Kim MH, Moon SH, et al. The combined measurement of total serum IgG and IgG4 may increase diagnostic sensitivity for autoimmune pancreatitis without sacrificing specificity, compared with IgG4 alone. *Am J Gastroenterol*. 2010;105:1655-1660.
14. Yu D, Vinuesa CG. The elusive identity of T follicular helper cells. *Trends Immunol*. 2010;31:377-383.
15. Kim H, Verbinnen B, Tang X, Lu L, Cantor H. Inhibition of follicular T-helper cells by CD8(+) regulatory T cells is essential for self tolerance. *Nature*. 2010;467:328-332.
16. Boulanger E, Fuentes V, Meignin V, et al. Polyclonal IgG4 hypergammaglobulinemia associated with plasmacytic lymphadenopathy, anemia and nephropathy. *Ann Hematol*. 2006;85:833-840.
17. Malisan F, Brière F, Bridon JM, et al. Interleukin-10 induces immunoglobulin G isotype switch recombination in human CD40-activated naive B lymphocytes. *J Exp Med*. 1996;183:937-947.
18. Gascan H, Gauchat JF, Aversa G, Van Vlasselaer P, de Vries JE. Anti-CD40 monoclonal antibodies or CD4+ T cell clones and IL-4 induce IgG4 and IgE switching in purified human B cells via different signaling pathways. *J Immunol*. 1991;147:8-13.
19. Pène J, Gauchat JF, Lécart S, et al. Cutting edge: IL-21 is a switch factor for the production of IgG1 and IgG3 by human B cells. *J Immunol*. 2004;172:5154-5157.

Table 1: Weight and laboratory data before (M0) and 1, 6, 12 and 18 months following rituximab administration.

	Normal reference Range	**Before treatment**	**Time after rituximab administration**			
		M 0	M 1	M 6	M 12	M18
Weight (kg)	75	55	56	66	70	70
Biological findings						
Hemoglobin (g/dL)	12 - 18	8.9	10.3	12.9	13.4	12.8
Alkaline phosphatase (U/L)	30- 115	369	255	86	116	91
Gamma-glutamyltransferase (U/L)	< 50	207	157	24	22	24
TSH (mIU/L)	0.3 - 3.6	8.1	-	4.2	1.96	-
Serum creatinine (mg/dL)	0.5-1.01	1.58	1.05	1.01	1.07	1.00
eGFR* (mL/min/1.73m²)	> 60	42	67	70	66	71
Proteinuria (g/day)	< 0.15	1.5-2.5	1.5	0.28	0.35	<0.15
Serum Electrophoresis						
Protein (g/dL)	6.5 – 7.5	11.9	9.5	8.3	8.7	8.0
Gammaglobulins (g/dL)	0.55 -1.1	8.4	5.17	2.65	2.64	2.53
Albumin (g/dL)	3.8 – 4.5	2.2	-	3.93	4.14	3.85
Serum IgG levels** (mg/dL)	660– 1240	8100	5100	2780	2470	2390
IgE levels (IU/ml)	< 150	1295	-	-	-	744
Serum IgG subclass***						
IgG1 (mg/dL)	400 - 980	6000	4200	2320	1740	-
IgG2 (mg/dL)	60 - 590	330	440	425	340	-
IgG3 (mg/dL)	18 - 80	1950	1530	115	100	-
IgG4 (mg/dL)	<1 - 160	1750	830	140	56	-

* eGFR was calculated using 4-variable Modification of Diet in Renal Disease (MDRD) Study equation.

****** Serum IgG levels were measured by nephelometry.

******* Serum IgG subclass levels were measured by competitive ELISA with monoclonal antibodies (ref. 8). Normal ranges are given for healthy adults. The normal range levels of IgG4 are given for males.

Note: Conversion factors for units: hemoglobin in g/dL to g/L, x10; serum creatinine in mg/dL to µmol/L, x88.4; eGFR in mL/min/1.73 m² to mL/s/1.73 m², x0.01667; serum protein in g/dL to g/L, x10; serum gammaglobulins in g/dL to g/L, x10; serum albumin in g/dL to g/L, x10; serum IgG levels in mg/dL to g/L, x0.01; and serum IgG subclass in mg/dL to mg/ml, x0.01. No conversion necessary for alkaline phosphatase (U/L), gamma-glutamyltransferase (U/L), thyroid stimulating hormone (mIU/L), and proteinuria (g/day).

Abbreviations: eGFR, estimated glomerular filtration rate; TSH, thyroid-stimulating hormone.

Table 2 : The hallmarks and clinical spectrum of IgG4-related systemic disease (IgG4-RSD) (ref. 1-7).

THE HALLMARKS OF IgG4-RSD	
1- Histological hallmarks - pronounced IgG4+ polyclonal plasma cells and T lymphocytes infiltration of various organs - sclerosis and obliterative phlebitis. **2-** Biological hallmarks - high IgG4 serum level (≥ 135 mg/dL) - increased serum IgG level (≥ 1800 mg/dL) - hypergammaglobulinemia (≥ 2.0 g/dL) without monoclonal component - +/- increased serum IgE **3-** Presence of auto-antibodies (including antinuclear antibodies and rheumatoid factor) - without definite auto-immune disorder - anti-SS-A/SS-B antibodies are almost always negative **4-** Marked improvement with steroid therapy	
THE CLINICAL SPECTRUM OF IgG4-RSD	
Pancreas	- Autoimmune pancreatitis (type 1), chronic sclerosing pancreatitis.
Hepatobiliary system	- Stricture of the bile ducts, Sclerosing cholangitis - Sclerosing cholecystitis - Hepatic "inflammatory" pseudotumor", IgG4-hepatopathy
Lymph nodes	- Lymphadenopathy with at least five histological subtypes: - Castleman's disease-like morphology - Reactive follicular hyperplasia - Interfollicular plasmacytosis and immunoblastosis - Progressive transformation of germinal center-like - Inflammatory pseudotumor-like
Salivary and lacrimal gland	- Sclerosing sialadenitis (Küttner tumor), Mikulicz disease - Sclerosing dacryoadenitis
Kidney	- Tubulo-interstitial nephritis - Pseudo-tumors of the kidney - Membranous nephropathy
Retroperitoneum	- Retroperitoneal fibrosis with obstructive uropathy
Thyroid gland	- Chronic thyroiditis, subclinical hypothyroidism
Mesentery, Aorta, and Mediastinum	-Multifocal fibrosclerosis -Sclerosing mesenteritis, mediastinal fibrosis -Periaortitis, Inflammatory aortic aneurysm
Lung and Pleura	- Interstitial pneumonia, nodular lesions
Stomach and Colon	- Chronic gastritis - Chronic (+/- ulcerative) colitis
Prostate	- Sclerosing prostatitis
Central nervous system	- Sclerosing Hypophysitis, pachymeningitis
Other lesions	- Inflammatory and sclerosing pseudo-tumors (liver, kidney, orbit, breast, lung, and brain…)

Figure 1 Legend:

(A) Histological and immunohistochemical analyses of lymph nodes from the patient and a control with lymphoid follicular hyperplasia. Hematoxylin and eosin staining (HE, original magnification, x 200) showed lymphoid follicular hyperplasia in both the patient's axillary lymph node and a control patient with HIV infection. Another non metastatic lymph node from a patient with colonic cancer was analyzed as a control and showed similar histological findings (data not shown)). B-lymphocytes, plasma cells, and T-lymphocytes were labeled for CD20, CD138, and CD3, respectively, and for CD4, and CD8 markers. Immunostaining for intracytoplasmic IgG subclasses was performed using monoclonal antibodies directed to human IgG1, IgG2, IgG3 and IgG4 (clones 4E3, HP6014, ZG4 and MC011, diluted 1:10, 1:10, 1:10000 and 1:200, respectively). Numerous CD138+ plasma cells were present, as compared with controls, most of which were located in the interfollicular regions (64% of nucleated cells). Immunostaining for intracytoplasmic IgG subclasses demonstrated that most plasma cells in the interfollicular zones contained either IgG3 (42.8%) or IgG4 (57%), which was not observed in the controls (data not shown). The topography of CD3+ T-cells was quite unusual in the patient, as compared with controls, with most CD4+ T-cells (62%) infiltrating the light zones of germinal centers. CD8+ T-cells were also found in the germinal centers. These findings were not found in the two control patients with follicular hyperplasia.

(B) Histological and immunohistochemical findings in the renal tissue. Light microscopy (Masson trichrome (MT); original magnification x 100) revealed 16 glomeruli, three of which were fibrotic. The remainder 13 glomeruli were normal. Only 10-20% of tubules showed atrophic changes but no marked tubulitis. The interstitium showed diffuse and marked renal interstitial mononuclear cells infiltration consisting of CD3+ T- and CD20+ B-lymphocytes, and numerous CD138+ plasma cells representing 33.5%, 12% and 54% of the cells, respectively. Immunofluorescence study revealed no extracellular immunoglobulin deposits. Immunostaining for intracytoplasmic IgG1 (data not shown), IgG2 (data not shown), IgG3 (*inset*: original magnification, x 1000), and IgG4 (*inset*: original magnification, x 1000) subclasses, performed as in the axillary lymph node, revealed that most plasma cells stained for IgG3 (60.7%) and IgG4 (32.5%).

(C) Histological and immunohistochemical findings in the minor salivary gland tissue. Light microscopy (hematoxylin and eosin (HE); original magnification x 100) revealed periductal fibrosis with a similar infiltration of mononuclear cells consisting of CD3+ T- and

CD20+ B-lymphocytes, and plasma cells (staining for both *kappa* and *lambda* light chains, data not shown), which represented 40%, 10%, and 51% of the cells, respectively. Immunostaining for intracytoplasmic IgG1 (data not shown), IgG2 (data not shown), IgG3 (*inset*: original magnification, x 1000), and IgG4 (*inset*: original magnification, x 1000) subclasses revealed that most plasma cells stained for IgG3 (42%) and IgG4 (44%).

Figure 1 :

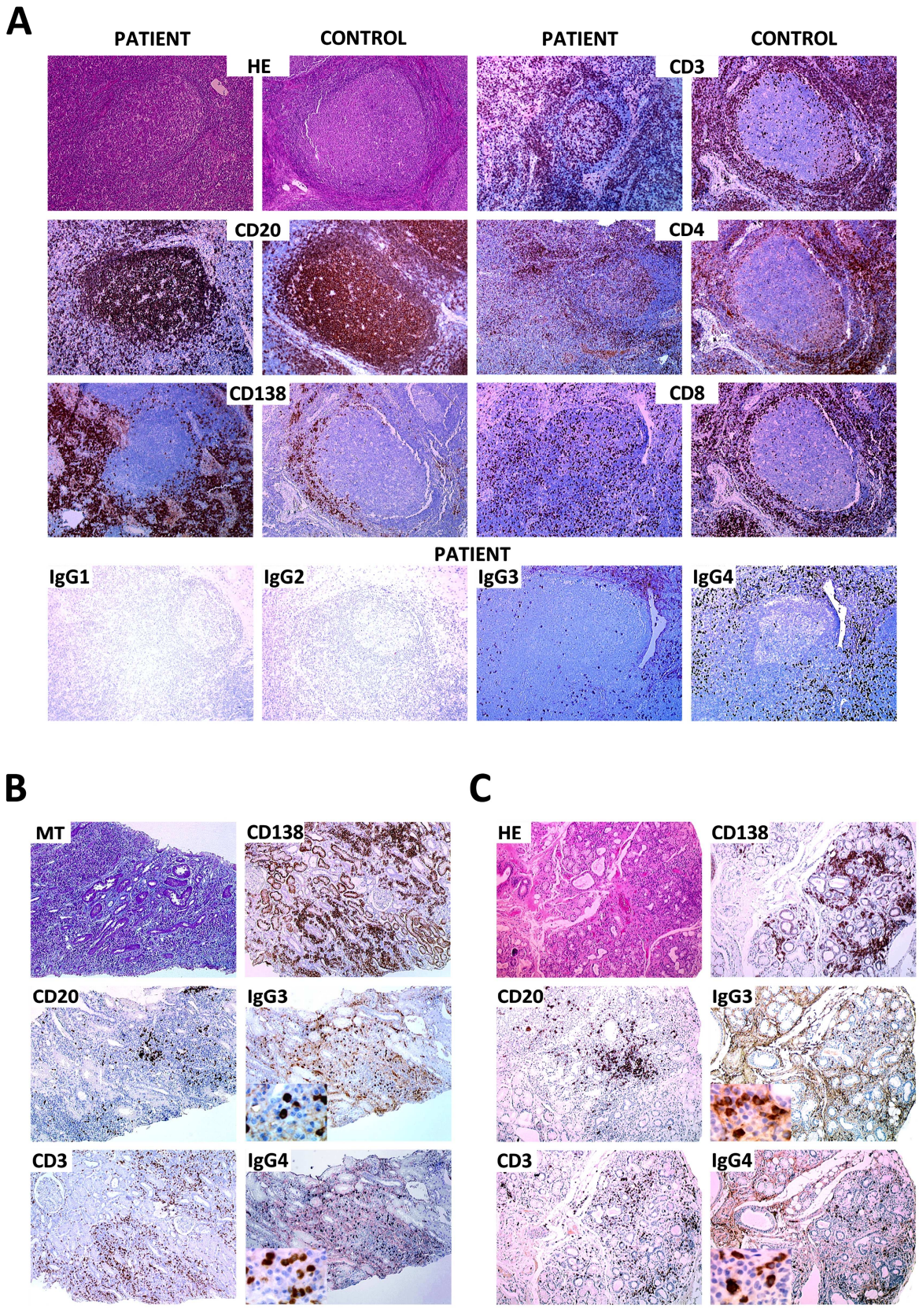
A
PATIENT
CONTROL
PATIENT
CONTROL
HE
CD3
CD20
CD4
CD138
CD8
PATIENT
IgG1
IgG2
IgG3
IgG4
B
MT
CD138
CD20
IgG3
CD3
IgG4
C
HE
CD138
CD20
IgG3
CD3
IgG4